Areas of enhanced ionization in the deep nightside ionosphere of Mars

F. Němec,[1,2] D. D. Morgan,[1] D. A. Gurnett,[1] and D. A. Brain[3]

Received 24 January 2011; revised 1 April 2011; accepted 8 April 2011; published 30 June 2011.

[1] We present observations of areas of enhanced ionization located in the deep nightside ionosphere of Mars as observed by Mars Advanced Radar for Subsurface and Ionospheric Sounding (MARSIS) on board the Mars Express spacecraft. Oblique ionospheric echoes coming from the same region observed during several consecutive MARSIS measurements enable us to constrain the geographic location of the reflection area that is the source of the echoes. We have identified 90 such events in all available data. None of the reflection areas are located in regions typically having a closed magnetic field line configuration. The locations of the reflection areas of enhanced plasma density are consistent with the ionization due to precipitating electrons on field lines connected to the collisional atmosphere. Reflection areas observed in regions of stronger magnetic field are found to have larger plasma number density. We use a model of Martian crustal magnetic field lines to demonstrate that the magnetic field has a "focusing" effect on incident particles. Electron impact ionization is thus expected to take place only in well-defined areas, in agreement with our observations. Our observations show that the deep nightside ionosphere of Mars is very irregular, controlled primarily by the configuration of crustal magnetic fields.

Citation: Němec, F., D. D. Morgan, D. A. Gurnett, and D. A. Brain (2011), Areas of enhanced ionization in the deep nightside ionosphere of Mars, *J. Geophys. Res.*, *116*, E06006, doi:10.1029/2011JE003804.

1. Introduction

[2] Our understanding of the formation of the nightside ionosphere of Mars is hampered by a dearth of nightside ionospheric observations. The deep nightside ionosphere located at solar zenith angles (SZAs) larger than 125° still remains basically unexplored [*Withers*, 2009; *Lillis et al.*, 2009].

[3] The Viking spacecraft and the radio occultation method were used by *Zhang et al.* [1990] to obtain ionospheric profiles at SZAs between 90° and 125°. For about 60% of these profiles, no significant peak could be identified, suggesting that the electron density in the nightside ionosphere is often too low to be detected. The average peak electron density for the remaining 40% of cases was about 5×10^3 cm^{-3} and the peak altitudes fell mostly in the range of 150–180 km. *Safaeinili et al.* [2007] used Mars Advanced Radar for Subsurface and Ionospheric Sounding (MARSIS) surface echoes to determine the total electron content (TEC) of the Martian ionosphere. Their results obtained for SZA range 100°–130° indicate that there is an enhancement in the TEC over regions where the magnetic field is vertical. Ionospheric reflections observed by the MARSIS instrument at SZAs between about 90° and 110° are very irregular and occur in highly localized regions [*Gurnett et al.*, 2008].

[4] More recently, *Němec et al.* [2010] analyzed MARSIS observations of the nightside ionosphere as a function of SZA, magnetic field magnitude and magnetic field inclination. They showed that at locations with weak crustal magnetic fields the occurrence rate of ionospheric densities that are substantial enough to be detected decreases with increasing SZA up to about 125°, suggesting that plasma transport from the dayside is an important source of ionization. At locations with strong crustal magnetic fields, the dependence on SZA is no longer apparent and the inclination of the magnetic field becomes a crucial parameter. Here the nightside ionosphere was found to occur preferentially in areas with nearly vertical magnetic field, i.e., in areas where the magnetic field configuration is most likely open. The apparent altitudes of peak electron densities derived from the MARSIS soundings were found to be too low to be realistic and oblique reflections were suggested as a possible explanation.

[5] *Fox et al.* [1993] discussed the importance of both electron precipitation and plasma transport from the dayside and derived upper limits for peak electron densities of the Martian nightside ionosphere. The computed electron density peaks were in the range 1.3–1.9 $\times$ 10^4 cm^{-3} and the peak altitudes were in the range 159–179 km. *Fillingim et al.* [2007] used an electron transport model and electron spectra observed by Mars Global Surveyor to investigate the

[1]Department of Physics and Astronomy, University of Iowa, Iowa City, Iowa, USA.
[2]Now at Institute of Atmospheric Physics, Academy of Sciences of the Czech Republic, Prague, Czech Republic.
[3]Space Sciences Laboratory, University of California, Berkeley, California, USA.

0148-0227/11/2011JE003804

effect of electron precipitation on the electron density in the nightside ionosphere of Mars. They calculated vertical profiles of the ionization rates and corresponding electron densities and demonstrated that the peak electron density can vary by a factor of about 3 depending on the electron spectrum used. The altitudes of peak electron densities were found to be within the range 156–166 km. Subsequently, a Monte Carlo method was used by *Lillis et al.* [2009] to investigate the coupled effects of crustal magnetic field gradients and pitch angle distributions (PADs) of precipitating electrons. Including such effects, particularly in the case of nonisotropic pitch angle distributions, was found to be essential in accurately predicting electron density profiles. However, the altitude of peak electron density was not much affected by crustal magnetic fields and/or electron PADs; it was near 160 km for all the analyzed cases.

[6] *Gurnett et al.* [2005], *Duru et al.* [2006] and *Nielsen et al.* [2007] used data obtained by MARSIS to identify oblique ionospheric echoes coming from regions of near-vertical crustal magnetic fields on the dayside of Mars. In the present study we report for the first time MARSIS observations of similar oblique reflections located in the deep nightside ionosphere of Mars (SZA > 125°). We demonstrate that the locations of reflecting areas can be constrained rather precisely and that they are in agreement with impact ionization by precipitating electrons.

[7] The instrument and data set used in this study are described in section 2. The results of our analysis of oblique ionospheric echoes are presented in section 3 and discussed in section 4. Section 5 contains a brief summary of the main results.

2. Data Set

[8] MARSIS is an instrument designed for topside ionospheric sounding on board the Mars Express spacecraft. The spacecraft is in an eccentric orbit around Mars with a periapsis altitude of about 275 km, an apoapsis altitude of about 11000 km, an orbital inclination of 86°, and an orbital period of 6.75 h [*Chicarro et al.*, 2004]. MARSIS uses a 40 m tip-to-tip electric dipole antenna for transmitting a sounding wave and for subsequent reception of its reflection from the ionosphere.

[9] Ionospheric sounding is based on the principle that, assuming no magnetic field, an electromagnetic wave of a given frequency f cannot propagate in areas where the plasma frequency f_p is larger than the frequency of the wave. Such a wave is reflected. Taking into account that in the case of Mars the electron gyrofrequency is generally much lower than the electron plasma frequency, the effect of magnetic field on the propagation of the sounding wave is negligibly small and the assumption above is valid. By measuring the time delay between the transmission of the wave and the time when the echo is received, it is possible to determine the range to the reflection point. By varying the sounding frequency f, it is possible to determine the range to the reflection point as a function of frequency. This dependence can be used to obtain a profile of electron density ranging from the satellite down to the altitude of peak electron density [*Morgan et al.*, 2008]. Finally, for vertical incidence at frequencies $f > f_p^{\max}$ signals do not undergo an ionospheric reflection. If not absorbed by the ionosphere, they generate surface reflections.

[10] During ionospheric sounding the MARSIS transmitter steps through 160 quasi-logarithmically spaced frequencies ($\Delta f/f \approx 2\%$) from 0.1 to 5.5 MHz. A quasi-sinusoidal pulse 91 μs long is transmitted at each step and the intensities of detected echoes are recorded in 80 equally spaced time delay bins over an interval of 7.31 ms. This corresponds to the resolution of the apparent range equal to about 13.7 km. A scan over all the 160 sounding frequencies lasts 1.26 s and it is repeated every 7.54 s. Taking into account the range of sounding frequencies used by MARSIS, the theoretical lower detection limit of the measurements of electron density is about 124 cm^{-3}. However, since the power radiated by the MARSIS antenna falls off rapidly at low frequencies, it is usually not possible to detect peak electron densities lower than about 5000 cm^{-3}. It is important to underline that this value is only approximate, there is no strict lower detection limit of the MARSIS instrument (see *Němec et al.* [2010, Figure 6a] for estimated probability of detection as a function of electron density). More detailed descriptions of the MARSIS instrument are given by *Picardi et al.* [2004] and *Jordan et al.* [2009].

[11] The principal output of the MARSIS instrument is a color-coded plot of the intensity of detected echoes as a function of the frequency f and the time delay t, called an ionogram. An example of an ionogram measured during orbit 2522 at 20:48:23 UT when the Mars Express spacecraft was in the deep nightside ionosphere at an altitude of 1002 km is shown in Figure 1. Two features can be seen in the ionogram. The first feature at frequencies from about 3 MHz up to the upper frequency limit of the instrument corresponds to the reflection from the surface of Mars [*Gurnett et al.*, 2005, 2008] and is not relevant to the topic of this paper. The second feature at frequencies from about 1 MHz up to 1.7 MHz at an apparent altitude of about 87 km is the echo due to the reflection of the transmitted pulse from the nightside ionosphere. As noted by *Němec et al.* [2010], time delays corresponding to nightside ionospheric echoes typically do not depend on frequency, which indicates a very "sharp" reflecting boundary. Consequently, it is possible to characterize them by their maximum frequency and the time delay of the echo (or the apparent altitude). It turns out that the apparent peak altitudes of nightside echoes are generally too low to be real. The most probable explanation is that these traces represent oblique reflections from the ionosphere [*Němec et al.*, 2010].

[12] Figure 2 represents an echogram corresponding to the deep nightside part of orbit 2522. It shows the intensity received in a fixed frequency range as a function of apparent altitude and time. The frequency range 1–1.5 MHz was chosen to approximately correspond to the nightside ionospheric reflection in Figure 1. The observed feature is due to the echo of the sounding signal from the nightside ionosphere. It can be seen that the apparent altitude of the feature increases with increasing time, from about 0 km shortly after 20:47:00 UT to nearly 130 km at the end of the analyzed time interval. It is unlikely that the real reflection altitude could change that much and, moreover, ionospheric peak altitudes below about 120 km are highly unlikely given what is known about the density profile of the Martian ionosphere. The only suitable explanation is thus an oblique

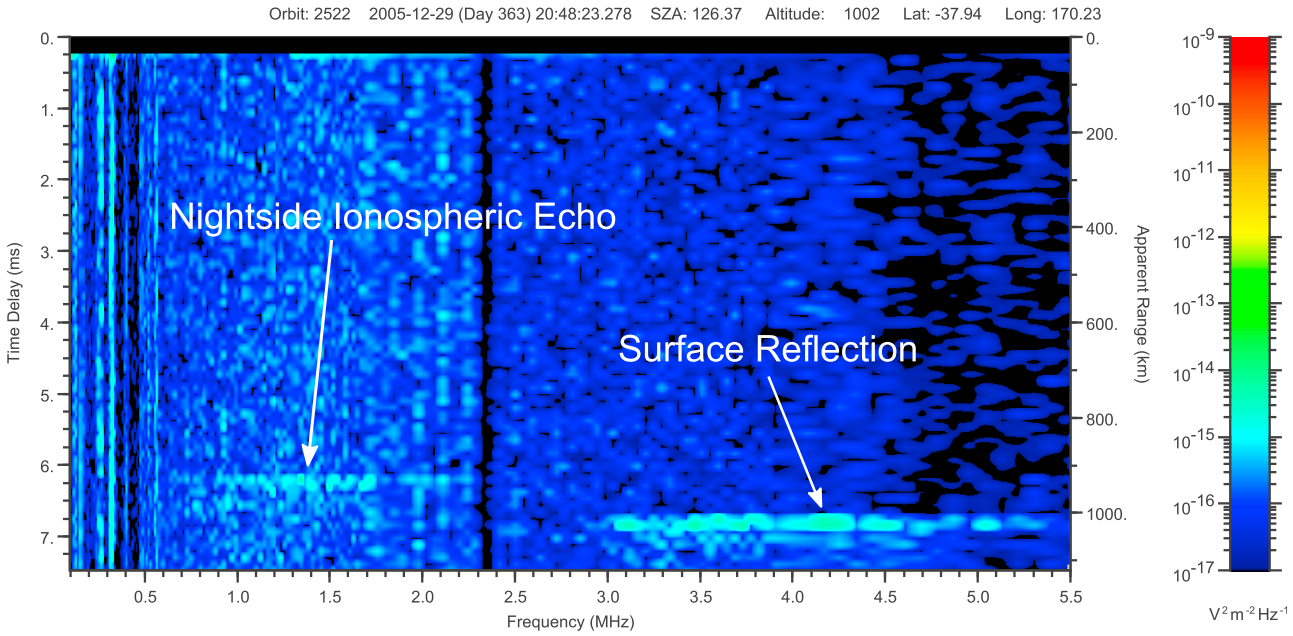

Figure 1. An ionogram containing a signature of the nightside ionosphere. Received intensity is color coded as a function of sounding frequency (abscissa) and time delay (left-hand ordinate) or apparent range (right-hand ordinate). The data were measured during orbit 2522 at 20:48:23 UT when the spacecraft was located at an altitude of 1002 km and SZA of 126.37°. The nightside ionospheric trace and surface reflection are labeled.

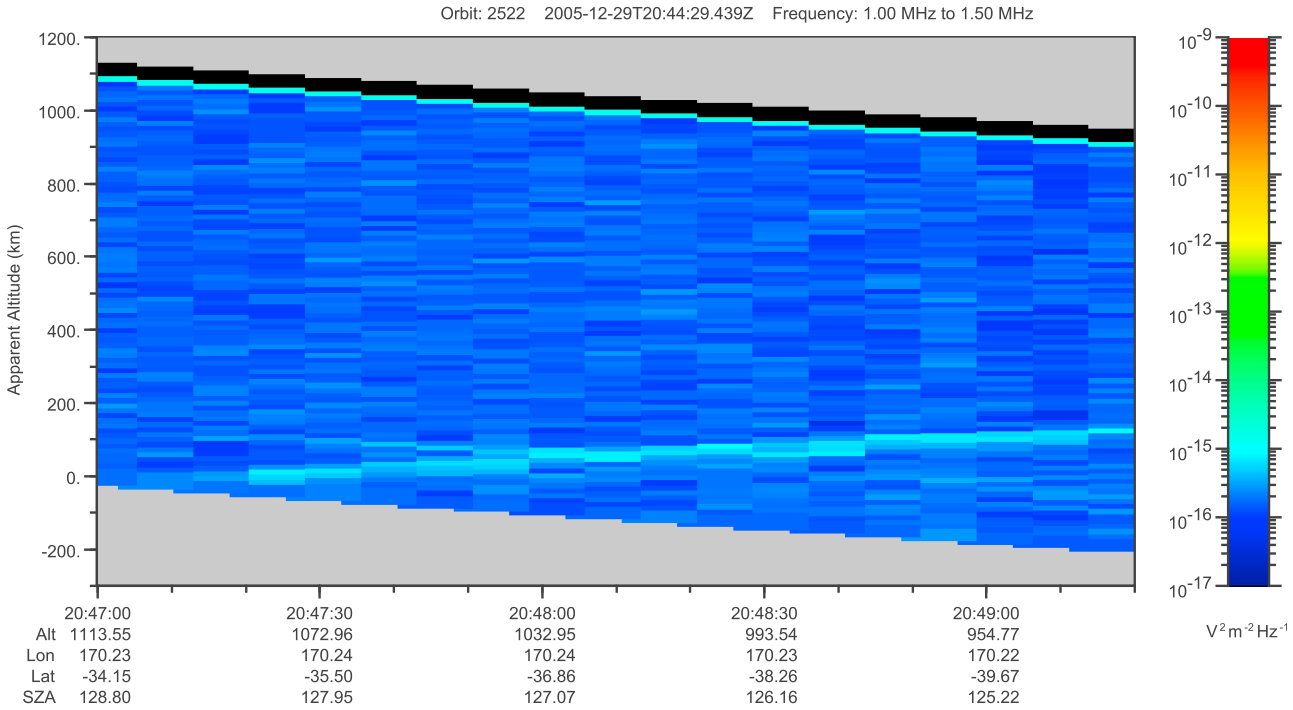

Figure 2. An echogram obtained for the frequency range 1–1.5 MHz showing the received intensity as a function of apparent altitude and time. Additionally, altitude (Alt), west longitude (Lon), latitude (Lat), and solar zenith angle (SZA) are shown in the bottom. The observed feature is due to the echo from the nightside ionosphere. The apparent altitude of the feature increases as the spacecraft approaches it and the reflection becomes more vertical.

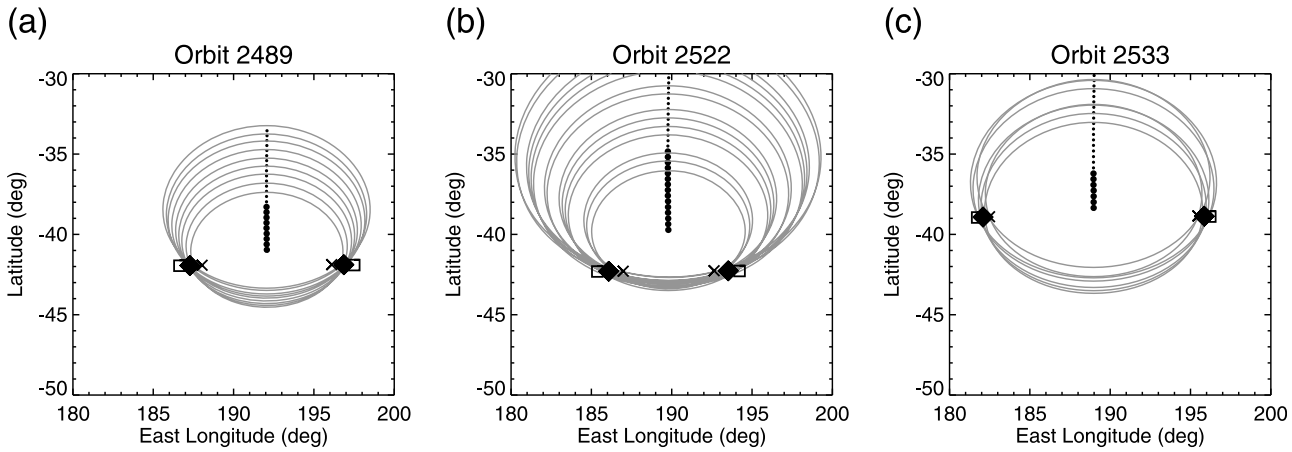

Figure 3. (a) Latitude-longitude map showing the possible reflection points determined for orbit 2489. Locations where MARSIS measurements were performed are shown by solid points. Small solid points correspond to the locations where no ionospheric reflections were detected. Large solid points correspond to the locations where ionospheric reflections were detected. For each of the ionospheric reflections the positions at 160 km altitude whose distance from the spacecraft location is equal to the apparent range are shown by circle-like curves. Possible reflection points determined using the least squares method are shown by solid diamonds. Possible reflection points determined assuming reflections at an altitude of 170 km are shown by squares. Possible reflection points determined assuming reflections at an altitude of 150 km are shown by crosses. (b) Same as Figure 3a but for orbit 2522. (c) Same as Figure 3a but for orbit 2533.

ionospheric echo from plasma that the spacecraft is approaching. Assuming that the reflections observed in a given time interval take place at the same very localized area, it is possible to determine its location by the analysis of several consecutive reflections similar to that performed by *Nielsen et al.* [2007].

[13] We have visually checked all the MARSIS data from the beginning of the mission until the end of September 2010 for the presence of deep nightside ionospheric echoes. Only the data measured at SZA > 125° were taken into account in order to minimize the influence of plasma transport [*Němec et al.*, 2010]. There were 1177 Mars Express orbits with at least some MARSIS data at SZA > 125°. Among these, 254 orbits contained at least one ionospheric echo. However, only events consisting of at least 5 consecutive ionospheric echoes were considered in the study, allowing us to determine the locations of reflection areas with a reasonable precision (see section 4). Altogether, 90 sets of nightside ionospheric reflections were accumulated.

3. Results

[14] The observations of the deep nightside ionosphere during orbit 2522 are interesting because they were performed at the time when MARSIS was in an area of strong and nearly horizontal crustal magnetic field. Consequently, no significant plasma transport nor impact ionization due to precipitating electrons is expected. However, there is a well pronounced ionospheric reflection observed above this area not only during orbit 2522, but also during orbits 2489 and 2533, i.e., the Mars Express orbits passing above the area just before and after (9 days before and 3 days after, respectively).

[15] Figure 3 shows the results of an analysis of possible reflection points determined for these three orbits. Latitude-longitude maps are presented separately for each orbit. Small solid points correspond to the locations where no ionospheric reflections were detected. Large solid points correspond to the locations where ionospheric reflections were detected. For each of these reflections, the apparent range from the satellite location to the reflection point is determined. Moreover, assuming that the altitude of the reflection point is equal to the peak ionospheric altitude, i.e., about 160 km [*Lillis et al.*, 2009], possible locations of the reflection point are represented by the ellipse-like curves. Note that in reality these are actually circles; however, due to the rectangular latitude-longitude projection used in Figure 3, they are slightly deformed. Finally, having observed ionospheric reflections in several successive MARSIS ionograms and assuming that they come from a single reflection point, it is possible to determine its location using the least squares method. Since the spacecraft projection is approximately a line, it is not possible to obtain a single solution. Instead, two different solutions exist, located symmetrically along the projection of the spacecraft orbit. Since the spacecraft is moving approximately in the north-south direction, the two solutions are symmetric about the north-south axis. We would like to emphasize that although we assume the peak ionospheric altitude to be equal to 160 km, the resulting location of the reflection point is not very sensitive to this choice. The results obtained for peak ionospheric altitudes equal to 150 km and 170 km are shown in Figure 3 by crosses and squares, respectively, and they are seen to agree closely with the results for 160 km.

[16] The locations of all the possible reflection points identified in Figure 3 are shown in Figure 4a. The individual symbols have the same meaning as in Figure 3. The fre-

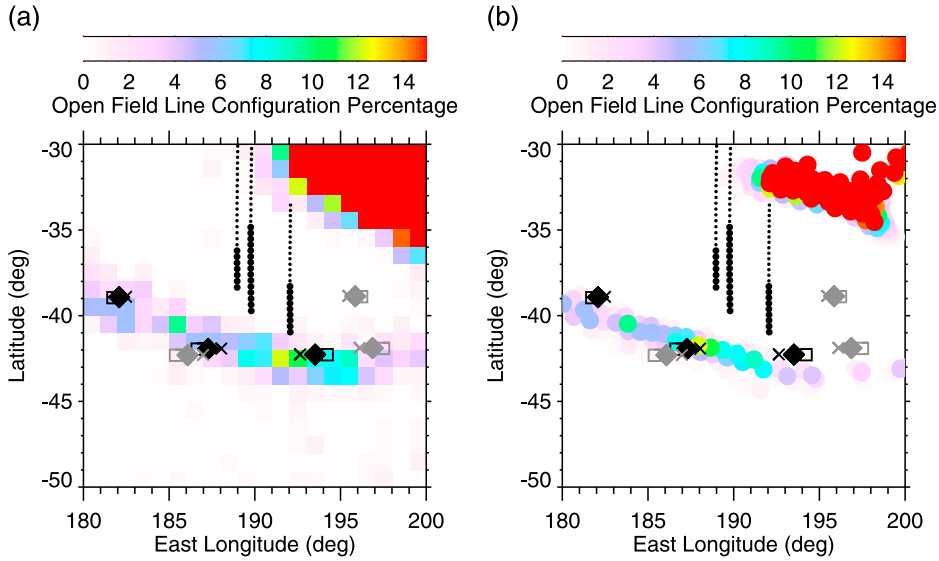

Figure 4. (a) Latitude-longitude map showing the locations of MARSIS measurements and possible reflection points for orbits 2489, 2522 and 2533. Meaning of individual symbols is the same as in Figure 3. The frequency of occurrence of open field line configuration at 400 km altitude adopted from *Brain et al.* [2007] is color coded. Locations of possible reflection points corresponding to the larger percentage of open field line configuration are plotted in black. Locations of possible reflection points corresponding to the lower percentage of open field line configuration are plotted in grey. (b) Same as Figure 4a but the open field line configuration percentage is traced along magnetic field lines to 160 km altitude.

quency of occurrence of open field line configurations at 400 km altitude and 02:00 LT of *Brain et al.* [2007, Figure 5f], is given by the color code in Figure 4a. The two possible reflection points obtained for each event are distinguished by the color used. Possible reflection points corresponding to the larger open field line configuration percentage are plotted in black, those for lower open field line configuration percentage are plotted in grey. Assuming that the localized reflection areas of enhanced plasma density are due to impact ionization by electrons precipitating along open magnetic field lines [*Fillingim et al.*, 2007; *Lillis et al.*, 2009], these areas are more likely to occur in regions with large open field line configuration percentage. Consequently, the reflection points plotted in black are more likely to be the true source of the reflection than those plotted in grey. We shall only consider the black points in the rest of this study. It can be seen that although the spacecraft only passed through areas of closed magnetic field configuration, the detected reflections come from a well defined region of open field line configuration to the south of the satellite. Curiously, no reflections coming from the region of possibly open field line configuration located to the northeast of the satellite were detected. Taking into account that the open field line configuration percentage in the region is only about 14%, this is most likely due to the magnetic field lines in this region being closed at the times of the measurements (see section 4 for a more detailed discussion of the variability of openness/closedness of magnetic field configuration).

[17] An additional complication stems from the fact that the frequency of occurrence of open field line configuration was determined by *Brain et al.* [2007] for an altitude of about 400 km, whereas the peak ionospheric altitude is about 160 km. This means that electrons entering in area of open magnetic field lines at an altitude of 400 km follow the magnetic field lines to low altitude and cause impact ionization. However, since the magnetic field is not exactly vertical the actual region where the ionization takes place is shifted slightly off the location at 400 km. In order to check this effect, we traced the magnetic field lines determined using the *Cain et al.* [2003] magnetic field model from an altitude of 400 km down to an altitude of 160 km. This enables us to plot in Figure 4b the frequency of occurrence of open field line configuration projected along the magnetic field lines to 160 km altitude. During the calculation, magnetic field lines with 1 degree resolution both in latitude and longitude were started at 400 km and traced down to 160 km. The resulting positions were then plotted by solid points in Figure 4b. One can see that the areas of open magnetic field line configuration are quite well localized already at 400 km altitude, but this localization becomes even more pronounced at 160 km. The incident electrons are focused into small precipitation areas (cusps).

[18] Having studied the ionospheric reflections observed above the specific area discussed above, we applied a similar analysis to all the available data. The results are shown geographically in Figure 5. The probable locations of individual reflection points are shown by crosses, where in each case we have eliminated one of the two possible reflection points determined from the ellipses. The frequency of occurrence of an open field line configuration at 400 km altitude is color coded in Figure 5a. Frequency of occurrence of an open field line configuration projected along magnetic field lines to 160 km altitude is color coded in Figure 5b. Black rectangles in the bottom part of the maps mark the area analyzed in Figures 3 and 4. The thickness of crosses corresponds to the peak electron density of events; the thicker

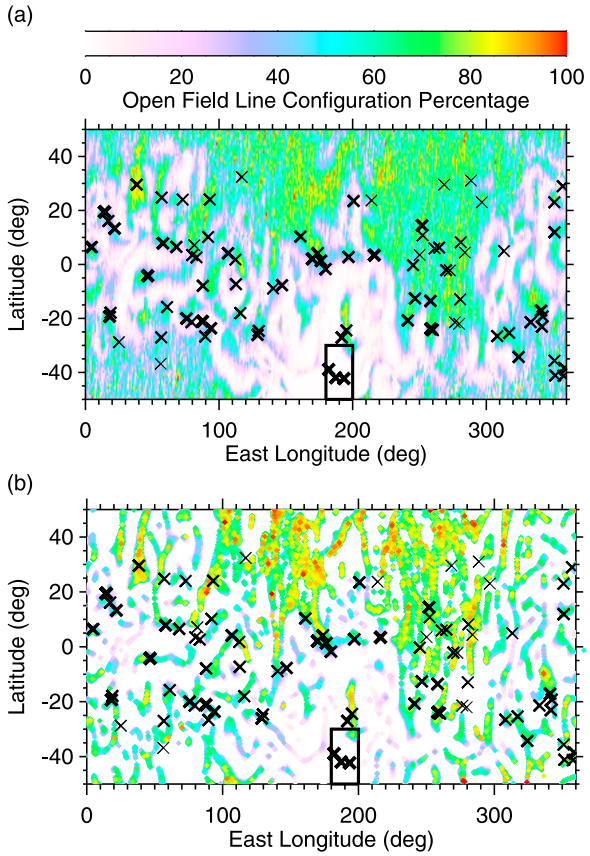

Figure 5. (a) Latitude-longitude map showing possible reflection points determined for all the events by crosses. The thickness of individual crosses corresponds to the peak electron density of a given event. The open field line configuration percentage at 400 km altitude adopted from *Brain et al.* [2007] is color coded. The black rectangle in the bottom part of the map marks the area analyzed in Figures 3 and 4. (b) Same as Figure 5a but the open field line configuration percentage is traced along magnetic field lines to 160 km altitude.

the cross is, the larger peak electron density. It should be noted that since the same event is observed during several MARSIS sounding intervals, several peak electron density measurements are available. However, they generally do not differ very much (not shown). The median observed peak electron density was taken as a measure of the peak electron density of a given event. It ranges from about 3.5×10^3 cm^{-3} up to about 5×10^4 cm^{-3}.

[19] Two main findings can be seen in Figure 5, generalizing the results obtained for the specific area presented above. First, the magnetic field has a focusing effect on precipitating electrons (see the color-coded frequency of occurrence of open field line configuration in Figure 5b as compared to Figure 5a). The localized areas of open field line configuration at 400 km identified by *Brain et al.* [2007] become narrower when projected to 160 km along magnetic field lines. Apart from this, the overall picture remains quite the same. It should be underlined once more that the tracing of magnetic field lines was done using the *Cain et al.* [2003] magnetic field model. This is expected to be reasonably precise in areas with strong crustal magnetic fields. However, it may be quite wrong in areas with weak crustal magnetic fields, because of the influence of the magnetic field induced due to the interaction with the solar wind (see section 4 for a more detailed discussion). The second notable feature observed in Figure 5 is that principally all the identified reflection points are localized in or very close to areas of open magnetic field line configuration. This can be seen especially well in Figure 5b. Most important, no reflection points are observed in areas with closed magnetic field line configuration. Finally, it seems that the reflection points are observed more likely at the edges of cusps rather than in their centers.

[20] The peak electron density of individual events as a function of the magnetic field magnitude predicted by the *Cain et al.* [2003] model at an altitude of 400 km is shown by crosses in Figure 6. A systematic increasing trend can be seen. The value of Spearman's rank correlation coefficient is equal to 0.60. This result indicates that the formation of areas of enhanced ionization by precipitating electrons requires not only an open magnetic field configuration, but also favors larger magnitudes of magnetic field.

4. Discussion

[21] In this study we have reported strong indications that the nightside ionospheric reflections observed by the MARSIS instrument are typically oblique rather than vertical. In particular, the minimum frequencies of surface reflections extend well below the maximum frequencies of ionospheric echoes [*Gurnett et al.*, 2008] and apparent altitudes of peak electron densities in the ionosphere are too low to be real [*Němec et al.*, 2010]. This predominance of oblique reflections indicates that the ionosphere is very "spotty" and irregular. For most of the time the satellite is located out of the regions of large electron density and the sounding signal does not get reflected from the ionosphere below. Moreover, even if there is a reflecting region of large electron density below the satellite, the sounding signal may be reflected out of the satellite location (if the isodensity surfaces are not strictly horizontal). The near absence of

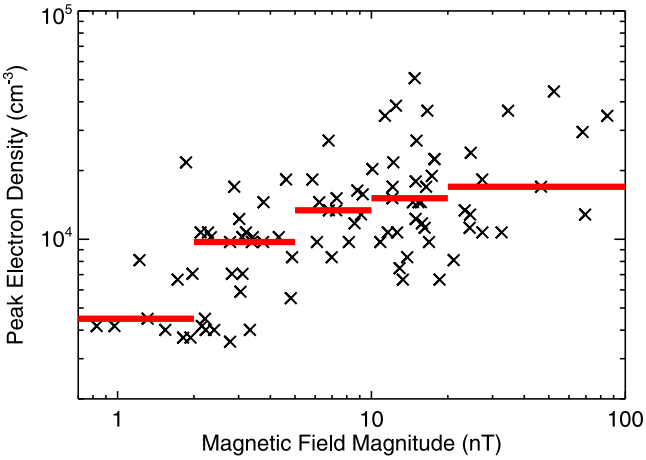

Figure 6. Peak electron densities of the identified events as a function of the magnetic field magnitude at an altitude of 400 km. Red lines show median values for selected abscissa intervals.

vertical echoes is rather different from the results of survey of dayside oblique reflections [*Duru et al.*, 2006], where the spacecraft was found to usually pass near or directly above the reflection point. The authors concluded that this indicates the presence of horizontal cylindrically shaped reflecting structures. This difference between our deep nightside results and dayside results of *Duru et al.* [2006] can be possibly explained in terms of difference in the nightside and dayside magnetic field configuration.

[22] Assuming that the reflections detected in several consecutive MARSIS measurements come from the same reflection point, i.e., from the same localized area of enhanced plasma density, it is possible to determine its location [*Nielsen et al.*, 2007]. There are two main reasons that we believe this assumption is valid. First, the regions of increased plasma density in the deep nightside ionosphere are probably very localized [*Fillingim et al.*, 2007; *Gurnett et al.*, 2008; *Němec et al.*, 2010]. Second, such an assumption seems to explain the observed data. In this study, we have seen that the ellipse-like curves in Figure 3, as well as in similar figures constructed for the remaining 87 events (not shown), intersect in very localized areas. If the approximation of a single reflection point was not valid, this would not be the case.

[23] Theoretically, two consecutive MARSIS measurements are sufficient to determine the location of the reflection point if its altitude is known and three consecutive MARSIS measurements are sufficient to determine the location of the reflection point and its altitude. However, the real situation is a bit more complicated. Most important, the resolution of the apparent range achieved by MARSIS is only about 13.7 km. Moreover, the procedure used to determine the location of the reflection point is not very sensitive to the peak altitude, as shown by the results obtained assuming the reflecting altitudes of 150 km, 160 km and 170 km plotted in Figure 3 [see also *Nielsen et al.*, 2007]. Consequently, it is not possible to use this procedure to accurately determine the altitude of the reflection point: the resulting altitude varies a lot with a minor change of the input parameters and cannot be considered reliable.

[24] However, it is possible to assume that the altitude of the reflection point is equal to some reasonable value. We assume that the altitude of the reflection point is 160 km, which corresponds approximately to the expected peak altitude of the nightside ionosphere [*Lillis et al.*, 2009]. This fixed value of the assumed altitude of the reflection point enables us, together with consecutive observation of the signal reflected from the same place during at least five MARSIS measurement intervals, to determine the location of the reflection point. The precision of this procedure is typically a few degrees in longitude and latitude (see Figure 3). As already mentioned, this procedure gives two equally valid results, symmetric about the path of the spacecraft. We have resolved this ambiguity by choosing the reflection point corresponding to larger open field line configuration percentage. Although this approach cannot explicitly distinguish the real reflection point, it enables us to choose the one which is more probable. Moreover, there is at present no other way to distinguish between the two points. The fact that we consider only events consisting of at least 5 consecutive echoes might possibly introduce some selection bias to our analysis, at least in the sense that the analyzed cases are "the best ones", with clear ionospheric echoes observable for a long time from different viewing angles. However, if we tried to change the required minimum number of consecutive echoes, our results remained generally the same.

[25] The locations of reflection points plotted in Figure 4 are in good agreement with the nightside areas of open field line configuration determined by *Brain et al.* [2007] at 02:00 LT. Namely, although the Mars Express spacecraft is in the area of strong and closed magnetic field at the time when the ionospheric reflections were detected, the reflections are coming from a localized region of open magnetic field line configuration located to the south of the satellite. It should be noted that nightside ionospheric reflections coming from this patch of ionization were detected above the area in orbits 2489, 2522 and 2533, i.e., in all orbits passing above the area between 20 December 2005 and 1 January 2006. No nightside ionospheric reflections coming from this region where observed in the remaining 19 satellite passes above the area. This can be probably explained in terms of the magnetic field configuration being open only during a limited period of time and closed otherwise. This is consistent with the results of *Brain et al.* [2007], who found that the frequency of occurrence of an open field line configuration in this region is only about 10%. Moreover, the IMF draping direction determined using the MGS spacecraft was very similar during all the three passes with nightside ionospheric reflections, providing supporting evidence for the explanation suggested above. Presently, our knowledge of the openness/closedness of magnetic field configuration is limited to the used average results parameterized only by geographic location [*Brain et al.*, 2007]. An analysis of the degree of openness of the magnetic field configuration as a function of the proxy IMF direction and the solar wind pressure needs to be done in the future to enable a more detailed explanation of when and where the areas of enhanced ionization occur in the deep nightside.

[26] Comparison of Figures 4a and 4b, derived using the magnetic field model of *Cain et al.* [2003] and assuming that electrons in the altitude range 160–400 km propagate along magnetic field lines, shows that the area of open magnetic field lines at 400 km altitude becomes even more localized at 160 km altitude. The radar reflection points occur along the region of open field line configuration located south of the satellite position. The physical picture corresponding to this situation is rather simple: plasma density is quite low everywhere except for a few localized regions. The frequency of the sounding signal transmitted from the spacecraft is consequently larger than the plasma frequency. The signal does not undergo any reflection until it meets the barrier of enhanced plasma density in the area of open field line configuration. There it gets reflected and, assuming normal incidence, propagates back to the satellite.

[27] The overall maps presented in Figure 5 demonstrate that the results obtained for the selected special area are systematic and valid all over the surface of Mars. Reflection points located in areas with an open field line configuration strongly suggest that the ionization in these regions is due to precipitating electrons. Moreover, they seem to occur at the edges of cusps rather than in their centers. This is in good agreement with the idea of an isolated ionization barrier

suggested above. Most important, there are no reflection points observed in areas where the magnetic field configuration is always closed. This means that all of the 90 deep nightside ionospheric observations analyzed in this paper can be explained by impact ionization due to electrons precipitating along the magnetic field lines in areas with an open field line configuration.

[28] One can see that while the largest open field line configuration percentage is in the northern hemisphere (where the crustal magnetic field is very weak), there are few events observed in this region. This is most probably due to the fact that *Brain et al.* [2007] were not able to unambiguously distinguish between converging open field lines that intersect the crust and nonconverging draped field lines that intersect the exobase. Their open field line configuration percentage therefore contains the total percentage for both these configurations. However, it is only the converging open field line configuration that is expected to result in a significant ionization (see below the discussion related to Figure 6). Since the field lines in weakly magnetized regions do not converge to the same degree as field lines near the crustal source [*Brain et al.*, 2007], this might be an explanation for the low number of ionospheric reflections coming from these regions. Finally, *Brain et al.* [2007] reported that the outer layers of regions of closed magnetic fields may contain trapped electrons (orange regions in Brain et al.'s Figure 8). However, their source terms are probably very small. Moreover, since most of these trapped electrons get magnetically reflected before reaching the altitude of peak ionization, they are not expected to cause any substantial ionization [*Lillis et al.*, 2009].

[29] As mentioned above, an additional minor complication stems from the fact that the electron measurements are performed at an altitude of about 400 km [*Brain et al.*, 2007], while most of the ionization is expected to take place at about 160 km [*Lillis et al.*, 2009]. We have tried to account for this by using the empirical magnetic field model of *Cain et al.* [2003] and tracing magnetic field lines from 400 km altitude down to 160 km. The Cain model was constructed using magnetic field measurements at 400 km altitude. The measurements included were primarily from the nightside in order to minimize the influence of the magnetic field induced due to the interaction with the solar wind. However, it is never possible to eliminate this influence entirely. Consequently, one can expect the magnetic field model to be rather accurate in areas of strong crustal magnetic fields. However, in areas with weak crustal magnetic fields the model values are probably much less precise. The same can be said about the tracing procedure, which entirely relies on the model magnetic field. Regardless of the relative precision of the magnetic field model, the effect of magnetic field tracing is primarily to improve the precision of our results, i.e., it causes the well localized areas of open field lines at 400 km to be even more strictly localized at 160 km altitude.

[30] The openness of the magnetic field configuration seems to be a necessary condition for the formation of the nightside ionosphere. However, Figure 6 suggests that once the magnetic field configuration is opened, it is the magnetic field magnitude that determines the peak electron density. Namely, the peak electron density in individual reflection areas is larger in areas with stronger magnetic field. This correlation is statistically very significant (Spearman's rank correlation is equal to 0.60 and the two-sided significance of its deviation from zero is equal to 2.8×10^{-10}, i.e., principally 100%).

[31] A proper explanation of why the electron density should be larger in areas with stronger magnetic field is difficult. We believe that this could be connected to the focusing effect of the magnetic field. The precipitating electrons propagate from high altitudes down toward the Martian surface following magnetic field lines. Although the original electron population can probably be assumed to be about uniformly distributed in area, the resulting distribution will be rather different. Basically, the more open magnetic field lines that lead to a given area, the larger the proportion of original population is expected to precipitate there. Taking into account that the number of magnetic field lines is proportional to the magnetic flux, i.e., to the magnitude of the magnetic field, this seems to explain the dependence observed in Figure 6.

[32] However, assuming that the initial pitch angle distribution of precipitating electrons is isotropic, stronger magnetic field regions also reflect more electrons. Consequently, there are two competing effects. One of them causes the number of precipitating electrons to increase as a function of magnetic field magnitude and one of them causes the number of precipitating electrons to decrease as a function of magnetic field magnitude. Since the electrons precipitating originally at low pitch angles are not expected to be reflected, our results might indicate that the pitch angle distribution of precipitating electrons causing ionization is primarily field aligned.

5. Conclusions

[33] A study of deep nightside (SZA > 125°) Martian ionosphere based on data from the MARSIS instrument on board the Mars Express spacecraft has been presented. We have focused on oblique reflections detected during several consecutive MARSIS measurements. Altogether, 90 events consisting of at least 5 consecutive ionospheric reflections were analyzed. It has been shown that they can be explained by assuming that each of them comes from a spatially very limited reflection area. Moreover, such an assumption enables us to determine the location of these reflection areas, corresponding to localized patches of enhanced ionization. They occur in regions with an open magnetic field configuration. No reflection areas located in regions with closed magnetic field line configuration were detected. This indicates that the ionization is due to impact ionization by electrons precipitating along magnetic field lines. Magnetic field lines have been traced down to the ionospheric peak altitude using an empirical magnetic field model, demonstrating that the magnetic field has a "focusing" effect. It has been shown that the events observed in regions of stronger magnetic field have larger peak plasma number density. Overall, we have shown that the deep nightside ionosphere of Mars is very irregular and controlled primarily by the configuration of crustal magnetic fields.

[34] **Acknowledgment.** The research at the University of Iowa was supported by NASA through contract 1224107 from the Jet Propulsion Laboratory.

References

Brain, D. A., R. J. Lillis, D. L. Mitchell, J. S. Halekas, and R. P. Lin (2007), Electron pitch angle distributions as indicators of magnetic field topology near Mars, *J. Geophys. Res.*, *112*, A09201, doi:10.1029/2007JA012435.

Cain, J. C., B. B. Ferguson, and D. Mozzoni (2003), An $n = 90$ internal potential function of the Martian crustal magnetic field, *J. Geophys. Res.*, *108*(E2), 5008, doi:10.1029/2000JE001487.

Chicarro, A., P. Martin, and R. Trautner (2004), The Mars Express mission: An overview, in *Mars Express: The Scientific Payload*, edited by A. Wilson and A. Chicarro, *ESA Spec. Publ.*, *ESA SP-1240*, 3–13.

Duru, F., D. A. Gurnett, T. F. Averkamp, D. L. Kirchner, R. L. Huff, A. M. Persoon, J. J. Plaut, and G. Picardi (2006), Magnetically controlled structures in the ionosphere of Mars, *J. Geophys. Res.*, *111*, A12204, doi:10.1029/2006JA011975.

Fillingim, M. O., et al. (2007), Model calculations of electron precipitation induced ionization patches on the nightside of Mars, *Geophys. Res. Lett.*, *34*, L12101, doi:10.1029/2007GL029986.

Fox, J. L., J. F. Brannon, and H. S. Porter (1993), Upper limits to the nightside ionosphere of Mars, *Geophys. Res. Lett.*, *20*(13), 1339–1342.

Gurnett, D. A., et al. (2005), Radar soundings of the ionosphere of Mars, *Science*, *310*, 1929–1933.

Gurnett, D. A., et al. (2008), An overview of radar soundings of the martian ionosphere from the Mars Express spacecraft, *Adv. Space Res.*, *41*, 1335–1346.

Jordan, R., et al. (2009), The Mars Express MARSIS sounder instrument, *Planet. Space Sci.*, *57*, 1975–1986, doi:10.1016/j.pss.2009.09.016.

Lillis, R. J., M. O. Fillingim, L. M. Peticolas, D. A. Brain, R. P. Lin, and S. W. Bougher (2009), Nightside ionosphere of Mars: Modeling the effects of crustal magnetic fields and electron pitch angle distributions on electron impact ionization, *J. Geophys. Res.*, *114*, E11009, doi:10.1029/2009JE003379.

Morgan, D. D., D. A. Gurnett, D. L. Kirchner, J. L. Fox, E. Nielsen, and J. J. Plaut (2008), Variation of the Martian ionospheric electron density from Mars Express radar soundings, *J. Geophys. Res.*, *113*, A09303, doi:10.1029/2008JA013313.

Němec, F., D. D. Morgan, D. A. Gurnett, and F. Duru (2010), Nightside ionosphere of Mars: Radar soundings by the Mars Express spacecraft, *J. Geophys. Res.*, *115*, E12009, doi:10.1029/2010JE003663.

Nielsen, E., X.-D. Wang, D. A. Gurnett, D. L. Kirchner, R. Huff, R. Orosei, A. Safaeinili, J. J. Plaut, and G. Picardi (2007), Vertical sheets of dense plasma in the topside Martian ionosphere, *J. Geophys. Res.*, *112*, E02003, doi:10.1029/2006JE002723.

Picardi, G., et al. (2004), MARSIS: Mars advanced radar for subsurface and ionosphere sounding, in *Mars Express: The Scientific Payload*, edited by A. Wilson and A. Chicarro, *ESA Spec. Publ.*, *ESA SP-1240*, 51–69.

Safaeinili, A., W. Kofman, J. Mouginot, Y. Gim, A. Herique, A. B. Ivanov, J. J. Plaut, and G. Picardi (2007), Estimation of the total electron content of the Martian ionosphere using radar sounder surface echoes, *Geophys. Res. Lett.*, *34*, L23204, doi:10.1029/2007GL032154.

Withers, P. (2009), A review of observed variability in the dayside ionosphere of Mars, *Adv. Space Res.*, *44*, 277–307.

Zhang, M. H. G., J. G. Luhmann, and A. J. Kliore (1990), An observational study of the nightside ionospheres of Mars and Venus with radio occultation methods, *J. Geophys. Res.*, *95*(A10), 17,095–17,102.

D. A. Brain, Space Sciences Laboratory, University of California, 7 Gauss Way, Berkeley, CA 94720, USA.

D. A. Gurnett and D. D. Morgan, Department of Physics and Astronomy, Office 718 Van Allen Hall, University of Iowa, Iowa City, IA 52242, USA.

F. Němec, Institute of Atmospheric Physics, Academy of Sciences of the Czech Republic, Bocni II 1401, Prague 14131, Czech Republic. (frantisek.nemec@gmail.com)